# Structure and Morphology of Nanocrystalline Calcifications in Thyroid

S.N. Danilchenko[1], A.S. Stanislavov[1], V.N. Kuznetsov[1], A.V. Kochenko[1], T.G. Kalinichenko[1],
A.V. Rieznik[2], V.V. Starikov[3], R.A. Moskalenko[2], A.M. Romaniuk[2]

[1] *Institute for Applied Physics, NAS of Ukraine, 58, Petropavlovskaya St., 40000 Sumy, Ukraine*
[2] *Sumy State University, 2, Rimsky-Korsakov St., 40007 Sumy, Ukraine*
[3] *National Technical University "Kharkiv Polytechnic Institute", 21, Frunze St., 61002 Kharkiv, Ukraine*

The paper presents the results of study on morphology, structure, elemental and phase composition of the calcified fragments from pathological formations of the thyroid gland. The X-ray diffraction and infrared spectroscopy revealed that all investigated pathological calcifications are represented by a defective carbonate substituted calcium apatite $Ca_{10}(PO_4)_6(OH)_2$. The use of transmission electron microscopy in combination with electron microdiffraction is shown to reveal some structural and morphological features of crystals of thyroid apatite, which are not detectable by other methods. Therefore, the local morphological and structural analysis of a mineral component of the deposits can be implemented both in one clinical case and in a wide variety of cases, if a delicate preparation at anatomical studies and sample preparation procedure will be applied.

## 1. INTRODUCTION

The deposition of pathological calcium-containing minerals (ectopic calcification) can occur almost anywhere in the human body [1-3]. Crystals of pathological deposits, as a rule, are of nanoscale sizes or even X-ray-amorphous [2] that complicates the study of their structure.

Calcifications formed in thyroid gland (TG) are more often associated with non-oncological changes of this organ, although there is opposite evidence [3-5]. Available today, information on the microstructure, elemental and phase composition of such mineral deposits is very limited. Moreover, specific crystallochemical characteristics of TG deposits related to one or another type of pathology remain unstudied. Implementation of such investigations should promote a deeper understanding of the processes of pathological calcification of TG and the ultimate development of a new strategy for the prevention and treatment of this type of pathology.

We should note that in the available literature, there is no clear and unambiguous classification of TG mineral deposits associated with certain clinical pathologies. Nevertheless, some authors have noted that calcification is most often observed in papillary thyroid carcinoma. At that, pathological biominerals can be attributed to psammoma bodies, stromal calcifications and/or ectopic bone formation [6]. Apparently, this classification cannot be considered as the final and only possible, especially since other types of TG pathologies accompanied by deposits of calcifications are also mentioned in many publications [for example, 7 and 8].

A special attention deserves questions of localization of mineral deposits of TG. Many authors emphasize the stable relationship between the features of pathology on the one hand and the localization and morphology of the accompanying calcifications on the other. However, the determination of the structural characteristics of a deposit of millimeter or micron scale is a serious problem. In these cases, it is necessary to apply local methods for studying the structure and composition with micron spatial resolution, which are available when using special

facilities coupled with synchrotron radiation sources [9]. At the same time, with proper preparation of the studied material, the significant results can be achieved by using traditional electron microscopy and electron diffraction. Besides the possibility of localization of the study area, electron diffraction in combination with electron microscopy has several important advantages compared with X-ray diffraction. The electron diffraction pattern can be matched with the microscopic image, i.e. morphological characteristics of crystalline particles, on which diffraction occurs. In the case, when crystalline particles are comparable with the electron probe size, it is possible to obtain the electron diffraction pattern from individual monocrystals and determine their crystallographic orientation [10].

The aim of the present work was to define the crystalline phase, structural characteristics, and morphological features of a mineral component of TG deposits. The accompanying problem was to reveal the specific differences between calcifications associated with different pathological types.

## 2. METHODS OF STUDY

In this work, we have studies 61 samples of pathological TG mineral deposits (in text Thyroid 1, etc.) with respect to their elemental and structural-phase composition as well as the morphological features of both the deposit as a whole (macro-level – increase up to 500) and individual crystalline particles (micro- and nano-levels). Anatomical, histomorphological and histochemical studies were preliminarily carried out for all presented clinical cases [11]. By the results of these works, the investigated samples were classified according to the TG pathology, on the background of which they arose: calcifications of malignant neoplasms (papillary, follicular and medullary thyroid carcinomas – 14 cases), benign neoplasms (thyroid adenomas – 30 cases), follicular adenoma (11 cases), goiter and pathological biomineralization, which occurs in thyroiditis (6 cases). When detecting any specific structural or concentration features of the calci-

fication, the clinical history and etiology of each sample could be easily established.

The mineral component was separated from soft tissues of the deposit by heat treatment in an electric oven (in air) at 200 °C during 1 hour. At that, there occurred the destruction of the organic part of the deposit and removal of free water while retaining constant structure of the mineral. After this low-temperature annealing, in the most cases it was easy to separate mechanically the solid mineral particles from the ash of organic tissues.

Investigation by scanning electron microscopy (SEM) was performed on the REMMA-102 (SELMI, Ukraine). This device allows to visualize the studied sample surface in a wide range of magnifications with a resolution of the order of 10 nm and obtain data on the elemental composition based on the analysis of the characteristic energy-dispersive X-ray (EDX) spectra excited by the electron probe. The processing of spectrometric information was performed using the standard software of the micro-analysis system.

X-ray diffraction study of the material structure was conducted on the diffractometer DRON-4-07 (Burevestnik, Russia) using Cu $K_\alpha$-radiation ($\lambda = 0.154$ nm) with the Bragg-Brentano focusing ($\theta$-$2\theta$) ($2\theta$ is the Bragg angle). The samples were taken in the continuous registration mode (at the speed of 2 °/min) in the range of $2\theta$ angles from 10° to 70°. The preliminary processing of the experimental results was carried out in the software package DIFWIN-1 (Etalon LLP), identification of the phase composition – by using the Joint Committee on Powder Diffraction Standards (JCPDS).

Infrared (IR) spectra were obtained on the Fourier-spectrometer Spectrum-One (Perkin Elmer, USA, 2003). Before the investigation, the samples in the powder form were mixed with the KBr powder (3 mg of the sample per 300 mg of KBr) and compressed into tablets. The measurements and analysis of the spectra were performed by using the standard software of the device.

Transmission electron microscopy (TEM) with electron diffraction (ED) was conducted on the device TEM-125K (SELMI, Ukraine), which allows to study the morphology and phase composition of crystalline particles of the calcification. When preparing the samples, annealed mineralized tissues in the powder form were placed in distilled water and treated with ultrasound using the facility UZDN-A (SELMI, Ukraine). Ultrasonic radiator was located in a vessel with distilled water and samples during 10 min. The specific power was approximately equal to 15-20 W/cm² at the radiator operating frequency of 22 kHz. A few drops of the obtained suspension were deposited on the directed vertically ultrasonic radiator UZDN-A and sputtered during 2-3 s varying the device power. The sputtered aerosol was caught on a thin carbon film (10-20 nm) located on a copper grid of the sample-holder. The micrographs and ED patterns were obtained with accelerating voltage of $U_{acc} = 90$ kV.

## 3. RESULTS AND DISCUSSION

According to SEM data, the mineralized material of the deposits represented nanoscale particles of arbitrary shape with signs of a brittle fracture along the edges. In a number of cases, one could observe large particles representing a resemblance to the mask (or mold) from the surface of TG soft tissues and repeating their shape (see

Fig. 1a, b, Thyroid 13 and Thyroid 14). As seen from the shown images, the mineral formed a solid shell (crust) or a crack with a smooth or fold surface on the TG surface, and the thickness of such a "crack" in some cases has a characteristic size (5-10 μm). It is of doubtless interest to determine the preferential crystallographic orientation of the mineral relative to the TG surface. In some cases, at large fracture growth, the porosity (sponginess, sponge structure) of the mineral deposits was observed (Fig. 1c, Thyroid 16).

In addition to the main lines of Ca and P, weak lines of S, K, Cl, and some other elements are often present in the EDX spectra. The ratio of the intensities of Ca and P lines is close to the characteristic ratio for the apatite
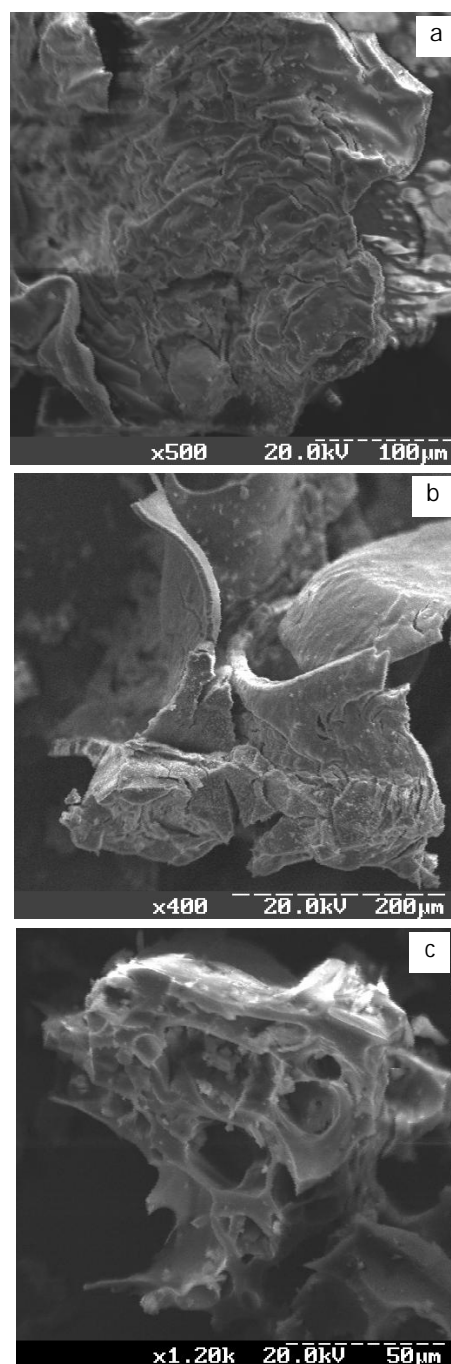


Fig. 1 – Morphological features of mineral particles of the TG deposits by the SEM data

$Ca_{10}(PO_4)_6(OH)_2$, although the spread of values is large enough and depends on the choice of the point of signal accumulation.

X-ray diffraction patterns of calcifications (Fig. 2a) are characterized by blurred and overlapping lines. The phase composition of the samples in most cases is represented exclusively by the apatite with different degree of crystallinity. In some cases (Fig. 2a), there are weak signs of the second phase – $\beta$-TCMP (tricalcium magnesium phosphate). In many diffraction patterns, in the vicinity of $2\theta \sim 21\text{-}22°$, one can observe a halo (Fig. 2b) typical for the cuvette material, which can be caused by a small amount of the sample coating only the central part of the cuvette. For most samples, the estimation of crystallite sizes by Scherrer [12, 13] along the normal to the plane (0 0 2) gives the spread of values from 14 to 30 nm.

The data of IR spectroscopy agree well with the above presented results of the structural analysis and confirm the apatite nature of calcifications. Moreover, IR spectra (Fig. 3) demonstrate the absorption bands corresponding to carbonate substitutions in the apatite structure. The discovered carbonate apatite has preferentially the B-type signs, i.e. signs of partial substitution of phosphate ions by carbonate ions (absorption peaks in the vicinity of 870-875 cm$^{-1}$ and 1410-1420 cm$^{-1}$) [14].

TEM and ED data in comparison with the results of the above described methods differ by more variety and admit some variations of interpretations. Nevertheless,
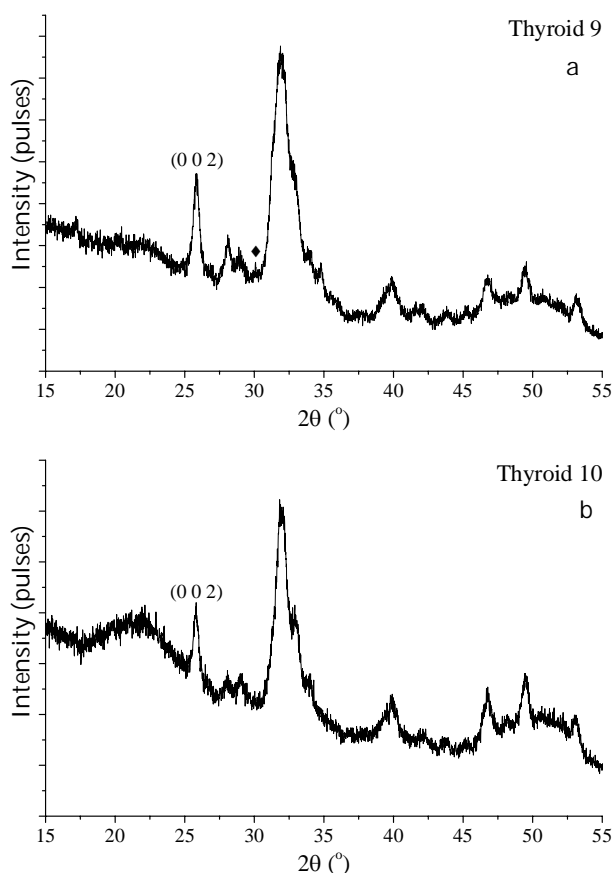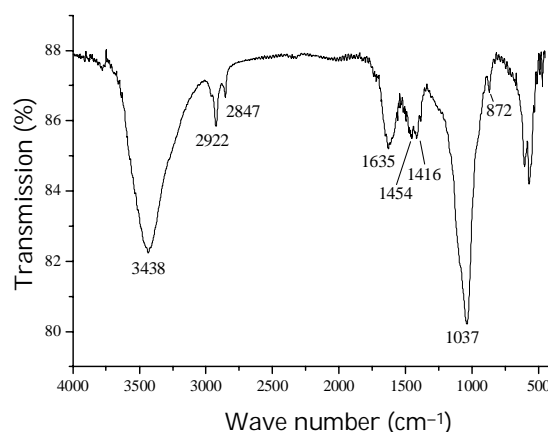


Fig. 3 – Typical IR spectrum of the TG pathological mineral

ED confidently confirms the presence of apatite in all studied TG deposits. According to TEM, apatite crystals can be approximately monodisperse or more often polydisperse; ED patterns are mostly polycrystalline, although there are features inherent to diffraction patterns from separate single-crystals. In a number of cases, the pronounced orientation of crystalline particles is evident with respect to the sample-holder substrate.

The micrograph in Fig. 4a illustrates a high degree of polydispersity of the crystals. The corresponding microdiffraction pattern (Fig. 4b) is also typical for the materials with different dispersity, when small crystals give a blurred ring (halo) and relatively large ones – individual reflections inherent to single-crystal ED. The halo in the ED pattern has discontinuities, which indicate a certain orientation (texture) of the reflecting crystallites. Small blurred reflections on the rings of the same radius correspond to the single reflexes (0 0 2). This implies a
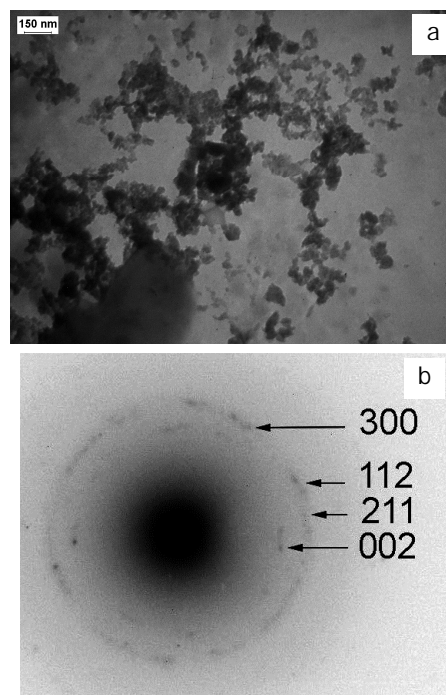


Fig. 2 – Typical diffraction patterns of the TG mineral deposits (sign ♦ denotes the main peak of $\beta$-TCMP, indexes *hkl* (0 0 2) designate the apatite line, from the broadening of which the crystallite sizes were estimated)



Fig. 4 – Electron-microscopic image of the crystals (a) and ED pattern (b) of the calcification sample (*Thyroid 8 / 34B*) (hereinafter, numbers on the ED pattern denote the *hkl* indexes corresponding to the apatite)

close crystallographic orientation of the relatively coarse crystals (occurred in the reflecting position) and small particles (which are on their surface or in the nearest-neighbor environment).

In another case (Fig. 5), in the electron-microscopic image one can see large crystals (up to hundreds of nm) surrounded by relatively small crystalline particles. The latter give in the ED pattern a blurred ring of merged lines with the Millers indices (2 1 1), (1 1 2), and (3 0 0), which correspond to close interpalnar distances (0.281-0.272 nm). Strong point reflexes with indices (0 0 2) and (0 0 4) are formed by a single-crystalline apatite particle with basal planes perpendicular to the observed surface.

Polydisperse apatite crystals are also typical for the case shown in Fig. 6. Large particles give point reflexes (see Fig. 6b), and small ones – blurred and merged rings from several reflexes close in interplanar distances. The absence of strong point reflexes with indices (0 0 2) is explained by the fact that coarse apatite particles with basal planes perpendicular to the image plane did not occur in the reflecting position. Taking into account the previous case (Fig. 5), one can assert that relatively large apatite crystals can be oriented/located by basal planes (of (0 0 l) type) both parallel and perpendicular to the plane of the observed surface.
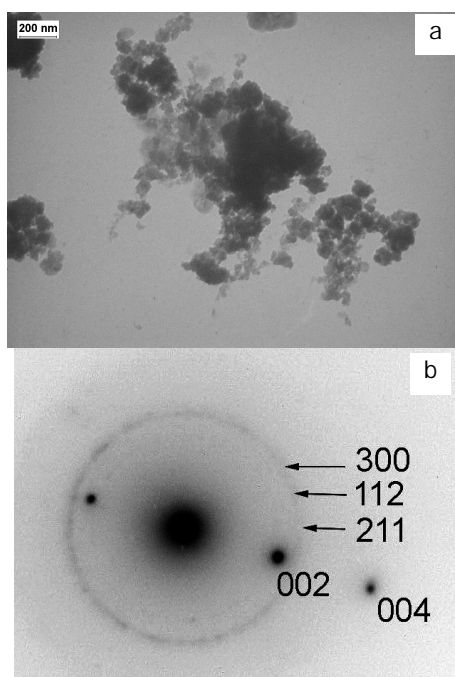


Fig. 5 – Electron-microscopic image of the crystals (a) and ED pattern (b) of the calcification sample (*Thyroid 10*)
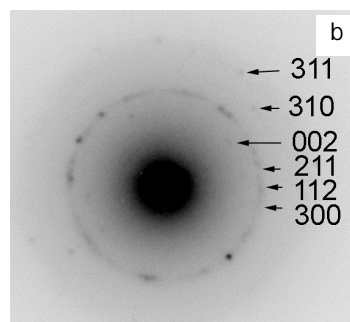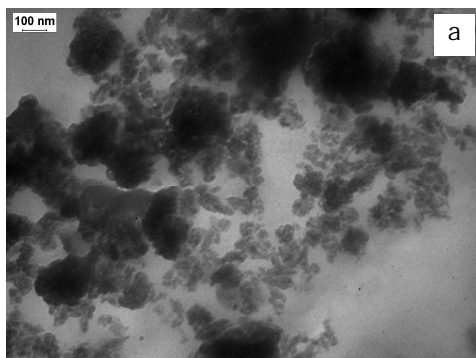


Fig. 6 – Electron-microscopic image of the crystals (a) and ED pattern (b) of the calcification sample (*Thyroid 13*)
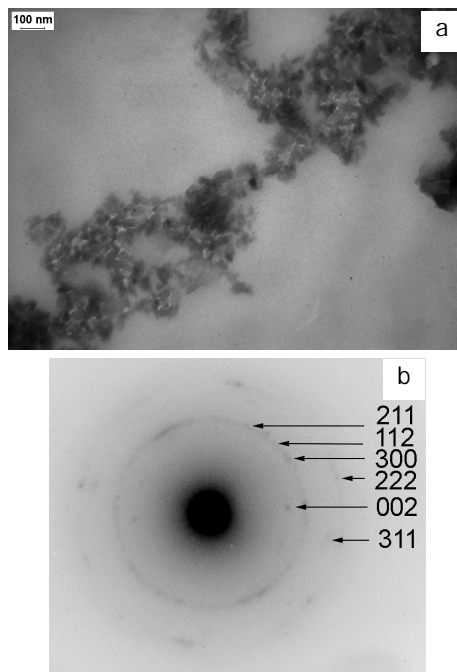


Fig. 7 – Electron-microscopic image of the crystals (a) and ED pattern (b) od the calcification sample (*Thyroid 24*)

In Fig. 7 we present the case of fine apatite particles. There are signs of preferential orientation: in the electron-microscopic image (Fig. 7b) one can see the chains of crystals, and in the ED pattern – alternating discontinuities and thickenings of diffraction rings.

The data represented demonstrate a wide variety of sizes, shape, and orientation of crystals of the TG calcifications, although they confirm their phase belonging to calcium apatites. Since the studies by TEM and ED methods do not require a greater amount of the sample material (compared with X-ray diffraction), it is possible to conduct investigations to reveal the structural and morphological features of the calcification in connection with its localization place in the pathological formation or in the TG in a whole.

## 4. CONCLUSIONS

According to the data of complex studies (X-ray and electron diffractions, IR spectroscopy), TG pathological calcifications are the nanocrystalline defective calcium apatite with a significant fraction of carbonate substitutions in the lattice (in positions of phosphate ions). The visible signs of other crystalline phases have not been revealed. The size of apatite crystallites determined from

the width of the X-ray diffraction peaks (0 0 2) belongs to a wide range, but for most samples it is equal to 14-30 nm. Stable relationships between the X-ray diffraction and IR spectroscopy data on the one hand and pathology type (the place of the deposit localization) based on the data of anatomical studies on the other hand have not been discovered.

The investigation of the morphological features of the deposits by SEM method at small magnifications (up to 500) has shown that the mineral can form a solid shell (crust) or a crack with a smooth or fold surface on the TG surface, and the thickness of such a "crack" in whole has the characteristic size (5-10 μm).

Based on the TEM data, the crystalline particles of calcifications, as a rule, are polydisperse (different-sized) and the spread of their sizes can be quite large. However, almost each sample has its own specific features concerning the morphology and sizes of the crystals as well as the ED pattern formed by them. Within this framework,

under the conditions of fine preparation of the initial material with the mechanical separation of the localized microcalcifications, it is possible to study the dependences of the TEM and ED data on the place of localization of the deposit or the type of clinical pathology. This is supposed to be the subject of further study. The results of this work will facilitate the development of instrumental approaches of solid-state physics and modern materials science to the study of the biological mineralogy objects determining the health and quality of human life.

## ACKNOWLEDGMENTS

## REFERENCES

1. T. Kirsch, *Curr. Opinion Orthopedics* 18, 425 (2007).
2. L. Stork, P. Müller R. Dronskowski, J.R. Ortlepp, *Z. Kristallogr.* 220, 201 (2005).
3. M.L. Khoo, S.L. Asa, I.J. Witterick, J.L. Freeman, *Head Neck* 24, 651 (2002).
4. J.V. Johannessen, M. Sobrinho-Simoes, *Lab. Invest.* 43, 287 (1980).
5. J.L. Hunt, L. Barnes, *Am. J. Pathology.* 128, 90 (2003).
6. Y. Bai, G. Zhou, M. Nakamura T. Ozaki, I. Mori, E. Taniguchi, A. Miyauchi, Y. Ito, K. Kakudo, *Modern Pathology* 22, 887 (2009).
7. J. Lee, S.Y. Lee, S.H. Cha, B.S. Cho, M.H. Kang, O.J. Lee, *Thyroid* 23, 1106 (2013).
8. B.K. Kim, Y.S. Choi, H.J. Kwon, J.S. Lee, J.J. Heo, Y.J. Han, Y.-H. Park, J.H. Kim, *Endocr. J.* 60, 155 (2013).
9. H. Jin, K. Ham, J.Y. Chan, L.G. Butler, R.L. Kurtz, S. Thiam, J.W. Robinson, R.A. Agbaria, I.M. Warner, R.E. Tracy, *Phys. Med. Biol.* 47, 4345 (2002).
10. E.I. Suvorova, P.A. Buffat, *J. Microscopy* 196, 46 (1999).
11. R.A. Moskalenko, A.V. Rieznik, A.V. Gapchenko, H.G. Prokopyeva, A.S. Malceva, *World of Biology and Medicine* 3, 324 (2015).
12. H.P. Klug, L.E. Alexander, *X-Ray Diffraction Procedures: For Polycrystalline and Amorphous Materials* (New York: Wiley: 1974).
13. S.N. Danilchenko, A.V. Koropov, I.Yu. Protsenko, B. Sulkio-Cleff, L.F. Sukhodub, *Cryst. Res. Technol.* 41, 268 (2006).
14. T.I. Ivanova, O.V. Frank-Kamenetskaya, A.B. Kol'tsov, V.L. Ugolkov, *J Solid State Chem.* 160, 340 (2001).